Four-Scale Linear Model for Anisotropic Reflectance (FLAIR) for Plant Canopies.

II: Partial Validation and Inversion using Field Measurements

H. Peter White[1], John R. Miller[2], Jing M. Chen[3]

[1]Canada Centre for Remote Sensing, Natural Resources Canada, 588 Booth St., Ottawa, Ontario, K1A 0Y7

URL: http://www.ccrs.nrcan.gc.ca

[2]Dept. of Physics and Astronomy, York University, 4700 Keele St., Toronto, Ontario, M3J 1P3

URL: http://www.physics.yorku.ca

[3]Dept. of Geography, University of Toronto, 100 St. George St., Toronto, Ontario, M5S 3G3

URL: http://www.geog.utoronto.ca/info/facweb/Chen/jxiel/jChen_Home.html

Invited paper

Abstract – To address the need for a flexible model of the bidirectional reflectance distribution function (BRDF) that is also suitable for inversion, the **FLAIR** Model (**F**our-Scale **L**inear Model for **A**n**I**sotropic **R**eflectance) has been developed and reported in the literature [1]. Based on the more detailed Four-Scale Model of Chen and Leblanc [2], **FLAIR** is a linear kernel-like model, developed with the aim of not being limited to specific canopy characteristics or view/illumination geometry, while maintaining a direct relationship between canopy architectural properties and model coefficients. Having been previously demonstrated to have the ability to capture the bi-directional patterns in both forward and inverse modes of calculation, this paper examines this model in describing the boreal canopy by applying **FLAIR** to multi-angular data sets obtained by various sensors during BOREAS 1994. Effects of sensor field of view, ranges of view/solar illumination geometry, and multiple sensor use on BRDF derivation and inversion for canopy parameter retrieval are demonstrated.

Published in IEEE Transactions on Geoscience and Remote Sensing, vol. 40, no. 5, May 2002

I. INTRODUCTION

Efforts to monitor global vegetation cover and land surface broadband albedo have lead to extensive investigations of bidirectional reflectance characteristics of vegetative canopies; for example see [3], [4], [5], [6], [7], and [8]. As an increasingly detailed influx of data is produced, the need exists for a flexible model of canopy bidirectional reflectance suitable for inversion and that provides quantitative information about canopy architectural and reflectance characteristics that may be used for comparison to other canopies. One such model developed as a result of this is **FLAIR** (**F**our-Scale **L**inear Model of **A**n**i**sotropic **R**eflectance) [1], based on the Four-Scale Model of Chen and Leblanc [2].

The ability of **FLAIR** to model forest canopy reflectance has been demonstrated in part by comparing modelled results to those produced by Four-Scale [1]. Further, when the Four-Scale Model was used to simulate boreal forest canopy BRF data sets (used to validate the Four-Scale Model [2][6]), inversion with FLAIR provided BRF functions with coefficients that maintained a direct relevance to the canopy characteristics used to produce the simulated data. Application of FLAIR to data obtained from the spaceborne POLDER over Canadian boreal forests has also been demonstrated to provide realistic effective leaf area index, L_e (where $L_e = \Omega LAI$, the product of the canopy clumping index and the half total leaf area per unit horizontal ground area), and mean overstorey and background reflectance factors [9]. Additional validation and examination of FLAIR with data obtained by airborne CASI, POLDER, and PARABOLA sensors are performed here.

In short, the FLAIR model is a sum of contributions of four component constituents of the canopy, as described in [1] (and summarized in Appendix A). It is expressed as:

$$BRF = R_{zt} \times k_1 + R_{zg} \times k_2 + R_t \times k_3 + R_g \times k_4 \qquad (1)$$

Where: R_x are the four scene component mean reflectance factors (*zt*: shaded overstorey; *zg*: shaded background; *t*: sunlit overstorey; *g*: sunlit background), and

k_x are the viewed proportions of the four scene components contributing to the observed BRF, (see Appendix A). These are functions of the view/illumination geometry and the effective leaf area index.

Further, by separating shaded from sunlit contributions, FLAIR provides information on the multiple scattering contribution from both the canopy and diffuse sky. The ratio of sunlit to shaded reflectance factors (as discussed in [1]) is referred to here as the overstorey and understorey multi-scattering factors, C_mF_{dt} and C_mF_{dg}.

II. FLAIR APPLICATION TO CANOPY REFLECTANCE

During BOREAS 1994 [10][11], forest canopy reflectance measurements were collected within the northern and southern Canadian taiga biome regions. This was done with a variety of airborne sensors, including POLDER [6][12], PARABOLA [13][14], and CASI [15][16]. The aim is to examine the potential for extrapolation of each derived reflectance function from FLAIR inversion to allow quantitative comparisons between forest sites, and between temporal changes within a site. One aspect inherent within this study is the ability to relate information provided by a variety of remote sensing instruments. Individual sensors each have unique angular and spectral resolutions, and are subject to view/illumination geometry limitations based on sensor location, deployment characteristics, and timing. Thus each sensor provides a uniquely limited measure of the surface reflectance variations. FLAIR was used to derived inverse functions from BRF observations from each of the three sensors, allowing between-detector and between-site comparisons of the ability to invert measured BRF to obtain a reflectance function and obtain canopy characteristics.

Inversion was performed on each spectral channel individually, with the derived parameters determined by the minimum constraint volume outlined in [1]. Multiple results occurred in some simulations. In many cases, especially for red spectral bands, these additional results included multi-scattering ratios of 0 or 1, with values of L_e less than 0.2 or larger than 5. Two effects were assumed to be contributing to this. First, in the red band, BRF values are generally low (<0.05) for boreal canopies. Sensor noise, atmospheric modelling accuracy, and natural variations in surface reflectance may contribute to prevent a quantitative measure of canopy BRDF for the range of view/illumination geometry available. In the near infrared (nir), derived reflectance factors and L_e were more consistent with measured values from various published studies. At these longer wavelengths, natural variations in surface reflectance and the influence of atmospheric scattering on the remotely sensed signal is less significant relative to the magnitude of the surface reflectance.

Secondly, multiple scattering characteristics in the overstorey and background levels should be similar in magnitude. Having shaded overstorey receive almost no contribution from canopy multiple scattering and diffuse

sky, while shaded background areas receive significant contributions is not realistic, and does not match previous attempts to measure these levels [16][17]. An additional constraint was thus included to the inversion algorithm, where $C_m F_{dt}$ and $C_m F_{dg}$ are constrained such that the smaller value is within 50% of the larger. Further study of these contributions to the canopy BRF are needed to improve modelling efforts, and are been pursued [18].

Site biophysical parameters are then determined based on the minimum constraint volume that would simultaneously meet constraints imposed by the infrared BRF data and multi-scattering limits, and allow for successful (not optimal) inversion of the visible (red) BRF data. In some cases this minimum constraint volume occurred for a range of L_e. When this happened, the range of results are reported.

A. Applications to POLDER Data

During BOREAS 1994, the POLDER sensor was mounted aboard a C-130 airplane and repeatedly flown to obtain multi-view angle reflectance measures near the principal, perpendicular, and oblique planes relative to the Sun. Different spectral bands were acquired using a rotating filter wheel in the view path, the red and nir are examined here, centred at 670 nm and 864 nm with band widths of 20 nm and 40 nm respectively. The sensor was flown at an altitude of 1675 m a.g.l. (above ground level), providing ground pixel dimensions of 35×35 m^2 at nadir. Data was averaged to 3×3 pixels to reduce noise. The 6S algorithm [19] was used with a mid-arctic summer atmospheric model to characterize the atmosphere, allowing for the derivation of top of canopy reflectance from measured radiance values [6]. Data acquired on 21-July-1994, from a 900×900 m^2 area around each site were used. Functions were determined in the forward mode using values recommended by [2] and [6] (Table 1), and then by FLAIR inversion to obtain canopy properties (Figure 1). This data provides multiple view angle (multi-θ_v) BRF's for a single solar angle per site (uni-θ_i).

1) Old Black Spruce: Data acquisition occurred with θ_i = 33.5°. In this data set, the sensor was flown approximately 10° off the solar and cross-solar planes. When applying SSA-OBS nominal site architectural properties and reflectance factor values (Table 1) to produce canopy BRF, it was found that the forward modelled BRF curve reproduced the measured POLDER BRF values. Inversion of this data results in a function that also reproduces these values (Figure 1a). Note however that the inverse derived reflectance near the horizon starts to increase, resulting in a more 'bowl-like' appearance. Canopy parameters determined from inversion suggest a relatively bright overstorey and dark understorey, with a smaller L_e, than measured in the field. In the inversion of

this uni-θ_i data, the minimum constraint volume ranged between $1.20<L_e<2.46$. The upper limit of this range is similar to that reported by [6] of L_e=2.5. Within this range, resulting component mean reflectance factors slightly decreased with increasing L_e, also approaching values reported for this site. A summary is provided in Table 2.

2) Old Jack Pine: BRF measurements were obtained with θ_i = 35°. Here the sensor was flown closer to the solar and cross-solar planes, within 3° of each plane. When applying SSA-OJP nominal site values, it was found that the forward modelled BRF function reproduced this data (Figure 1b). The inverted FLAIR function also reproduced the general shape and magnitude in both the red and near infrared, with a more 'bowl-like' forescatter region. Biophysical parameters determined from inversion results in a darker overstorey and brighter understorey, with larger L_e, than measured in the field. Again, this uni-θ_i data provided a range of results, with $1.90<L_e<3.19$ (Table 2). In this case, the lower end of the range is more comparable to the value measured in the field (L_e=1.1). Within this range the inverse FLAIR derived reflectance factor values were generally noted to decrease with increasing L_e.

B. Applications to PARABOLA Data

With the PARABOLA sensor [13][14] three different spectral bands were acquired during BOREAS 1994, centred at 662 nm, 864 nm, and 1658 nm with band widths of 60 nm, 140 nm, and 200 nm respectively. An angular resolution of 15° was obtained with an altitude of ~25 m a.g.l. Partial data sets for the SSA-OBS and SSA-OJP sites were provided for this study. Field reflectance values of the canopy components at 1658 nm were not available for this investigation. Comparison between the multi-θ_i data and POLDER uni-θ_i data demonstrate two significant differences. In the forescatter region, a definite bowl shape is present in the PARABOLA data, but not with POLDER. In the backscatter region, the hot spot is less well defined by PARABOLA, often appearing to extend almost to the horizon. This is probably due in part to the increased angular field of view and wider bandwidths.

1) Old Black Spruce: Here the forward FLAIR modelled BRF (derived with the nominal parameters discussed above) over-estimate observed values in the forescatter region, and underestimate observed backscatter values (see Figure 2a for θ_i = 45°) for all θ_i. The inverse FLAIR functions better match the general shape and magnitude of the observed BRF, providing better correlation to the forescatter bowl feature. The unusually flat and bright backscatter regions recorded by this sensor are not well modelled by FLAIR. Inverse derived L_e is under-estimated, and reflectance factors are similar to field values (Table 3).

2) Old Jack Pine: When examining SSA-OJP data, forward FLAIR functions generally reproduce the shape and magnitudes of measured BRF, but underestimate the extent of the forescatter bowl feature. Inverse FLAIR functions better match this feature (Figure 2b). Neither function is able to reproduce the measured bright backscatter region. The bright near-horizon determined by the inverse function is due to FLAIR's attempt to fit a low hot spot feature with a bright backscatter plateau. To fit the forescatter region, derived background reflectance factors are decreased (Table 3) and multi-scattering contributions are increased relative to nominal field observations (Table 1).

PARABOLA is subject to a significant spectral (between 60 nm and 200 nm) and angular resolution (15°). This appears to 'flatten' the measured BRF around the hot spot, resulting in lower BRF and a plateau-like feature where the hot spot peak appears more like a hot spot plateau in the $\theta_v > \theta_i$, $\phi \sim 0°$ region. Note how the hot spot peak fits completely within one observational field of view. Also, as PARABOLA operated at a height of ~13 m above the top of canopy (25m above the ground), the ground footprint significantly changes in size, ranging from 9.1 m^2 at nadir to ~80 m^2 at θ_v=60°, with the average distance to the top of canopy changing from 13 m at nadir to 28 m. Such variations may result in poor sampling of the larger scale tree distribution (50 × 50 m^2) and shadowing effects modelled by FLAIR. The canopy gap probability is no longer a function of a tree groups, but becomes more related to small-scale tree distributions. At nadir the number of crowns viewed may range from a partial crown to as many as 3-4 trees, with up to 11 measurements performed for each view angle. Other observations at 2 m resolution have demonstrated that L_e can easily range ±1 within each BOREAS site [20].

Reported RMSE and correlation coefficients (Table 3) are calculated using all observed BRF's in the red, NIR, and MIR bands. With this range of view/illumination geometries, FLAIR inversion was able to converge for both canopies, however the spatial scale of the observations are not adequately modelled by FLAIR, which may explain the poor correlation of derived L_e with field measurements.

C. Applications to BOREAS-CASI Data

BRFs of the SSA-OJP site were obtained from 2 m resolution airborne multi-θ_v imagery taken at 1600 m a.g.l. during February FFC-W and August/September IFC-3 campaigns. The CASI was run in imaging mode, providing two bands for this study. During the winter campaign, bands were centred at 666 nm and 865 nm, with bandwidths of 16 nm and 25 nm respectively. For the late-summer campaign, bands were centred at 665 nm and 880 nm with bandwidths of 6 nm and 8 nm respectively. Atmospheric correction was performed using the Canadian Advanced

Modified 5S (CAM5S) [21]. BRF's were obtained by dividing the 1×1 km^2 region centred on the Tower Flux Site into 50×50 m^2 sub-sites, with each sub-site averaged to provide a mean BRF comparable to the POLDER data sets discussed above. Each sub-site view orientation (θ_v, ϕ_v) was determined using aircraft GPS and sensor pitch and roll, with θ_i, ϕ_i determined based on time of acquisition and site latitude and longitude [16]. The sixteen winter multi-angle acquisitions resulted in 5357 BRF values, while the six late summer acquisitions resulted in 1371 BRF values.

Unlike PARABOLA, BRF values taken from CASI spectral imagery have small angular widths (between 0.5° and 3° depending on sensor tilt) and small spectral bandwidths. This smaller spatial averaging does not significantly influence the magnitude and gradient of the BRF curve nearer the hot spot.

As no BRF is obtained at the hot spot during either CASI campaign, the forescatter bowl shape becomes the dominant influence in determining inverse FLAIR functions. Note the relative BRF increase at small scattering angles compared to POLDER and PARABOLA data. At large θ_i, FLAIR kernels indicate that there are significant contributions by shaded components to forescatter BRF [1], while sunlit components are uniquely significant contributors in the hot spot region only. With little BRF observed in this region, model inversion is expected to be less accurate in determining sunlit component reflectance values. Resulting BRF functions are provided in Figure 3.

1) Summer Old Jack Pine: BRF measurements were obtained with $50° < \theta_i < 68°$. In the forward mode, the derived FLAIR function does not reproduce the magnitude of the BRF near the hot spot (Figure 3a). The forscatter bowl region however is better defined. This may be due in part to the accuracy of atmospheric correction algorithms at lower sun angles; where multiple scattering becomes more complex, and as atmospheric azimuthal asymmetry was not applied. FLAIR inversion derives shaded reflectance factors similar to those determined by inversion for the other cases, with $L_e = 1.30$. Sunlit overstorey reflectance factors however are brighter than those determined with the other data sets, with lower multi-scattering ratios (Table 4). This results from the increased gradient in the forescatter hot spot region and lack of data nearer the hot spot and further in the backscatter region.

2) Winter Old Jack Pine: During February, the sun remains near the horizon in Canada, resulting in $69° < \theta_i < 77°$. During this campaign, field measurements of the background snow cover reflectance were performed [16], with a resulting nadir reflectance factor of ~0.85 for both red and nir bands being determined. When this value is used, forward FLAIR functions generally reproduce the CASI BRF winter observations (Figure 3b). Inversion results in a bright understorey, with an overstorey similar in reflectance to the summer inversion, low multi-scattering ratios,

and L_e = 1.46. Winter overstorey reflectance factors and L_e values similar to the summer inversion results demonstrates FLAIR's ability to separate the contribution of various canopy components to observed BRF subject to environmentally different conditions.

III. DATA SET COMPARISON

The time scale of the three campaigns provides a temporal baseline ranging from spring to mid-summer to late-summer and winter (for SSA-OJP), with PARABOLA (May-1994), POLDER (July-1994), and CASI (Sept.-1994; Feb.-1994) campaigns. This provides "snap-shots" of canopy BRF throughout one year. Observations of the background [16][17] and overstorey [6][22] during the May to Sept. growing period indicate minor changes occurred in the constituents' reflectance. Given this, observed BRF should be similar for each data set, subject only to the BRDF (assuming no sensor and calibration artefacts are present) and the presence of snow in the winter.

Comparisons of inverse FLAIR functions demonstrate similarities between sensors, with POLDER and PARABOLA data inversions resulting in comparable reflectance characteristics and overstorey L_e. However, limiting the data set to one θ_i (POLDER) can prevent FLAIR from converging upon one set of canopy parameters. When multiple θ_i (and θ_v) are used (PARABOLA, CASI) then FLAIR inversion is better able to converge upon a canopy description. This suggests that an increased range of both view and illumination orientations when obtaining canopy BRF's allow for better canopy characterizations, demonstrating the usefulness of multiple angle remote sensing of vegetated surfaces. Comparison between species after inversion of both POLDER and PARABOLA data suggests a slightly larger L_e for the jack pine site relative to black spruce. This is opposite to published field data [6][23] for these sites. High resolution measurements of overstorey density for these sites [20] suggest that L_e can vary up to ±1 within a few 10's of meters, thus sensor placement may be a contributing factor to this result.

Direct comparisons of the SSA-OJP canopy parameters derived from inversion have POLDER and PARABOLA data resulting in a denser, darker overstorey relative to CASI inversion results. Quantitative discussion of these values are limited due to the different band centres and widths for each sensor. In all three cases, observed BRF's provide well-defined forescatter regions, with only CASI data not including hot spot or backscatter observations. When using inversion results from one sensor to reproduce data observed at other sensor orientations (Figure 4), all resulting BRF functions reproduce the forescatter region with differences occurring in the magnitude of the hot spot, related to the model sensitivity in this region to the overstorey density and brightness. With CASI data inversion,

overstorey reflectance is determined by the BRF curve gradient in the forescatter region towards the hot spot, and not the backscatter BRF. Also, instrument field of view, band spectral width, and pointing accuracy can influence the measured hot spot and backscatter BRF. As suggested by the FLAIR kernels [1], accurate retrieval of overstorey reflectance and density depends in part on including accurate measurements of the BRF's in these regions.

IX. CONCLUSIONS

In this paper the FLAIR model was examined by inverting boreal forest BRF obtained by three different sensors during different seasonal conditions. Validation of FLAIR has been previously demonstrated with respect to the Four-Scale Model [1] and with space borne POLDER data [9]. As with many other existing linear kernel models, FLAIR has been demonstrated to: i) be able to utilize known canopy architecture characteristics and reflectance to model canopy BRF, and ii) use multi-angle reflectance measurements to produce canopy BRF functions applicable to a wide range of solar illumination/view geometries. Unlike these more traditional models however, FLAIR has also demonstrated the potential of iii) determining reasonable and quantitative canopy architectural and reflectance properties through inversion of multi-angle BRF measurements. Other models are also being developed with the potential for this capability (such as GHOST [24]), and a comparison between models will help further quantify the ability to use inversion to determine canopy properties.

When the boreal canopy data sets were examined, forward FLAIR functions were able to reproduce measured BRF to a high degree of accuracy (large r^2, low RMSE) with some discrepancies observed in the hot spot and backscatter region. These discrepancies appear related in part to sensor bandwidth and calibration characteristics, rather than to deficiencies in the FLAIR model.

Inversion provided functions that reproduced measured BRF. In these cases, inverse functions match the magnitude of the hot spot region for each sensor's observations, while maintaining the shape and magnitude of the forescatter region. Comparing results for each sensor individually demonstrates the model's ability to distinguish canopy component characteristics, allowing for monitoring of temporal changes within a site. The potential to compare characteristics between sites is also suggested, but was not sufficiently demonstrated here due to a lack of view/illumination orientations in the data, and in some cases to small spatial scales. FLAIR demonstrated improved ability to converge upon a canopy parameter set when a range of view/illumination geometry is used. When inverse functions derived from one data set are used to reproduce BRF's observed by other sensors (at different θ_i)

difficulties again arose with the magnitude of the hot spot not being properly reproduced. As this difficulty was not observed when using an individual sensor's data to produce BRF for various θ_i, spatial scale variations as well as sensor band centres and bandwidth and calibration characteristics are believed to be contributing influences.

APPENDIX A

The following is a summary of **FLAIR** [1]. Symbols are defined in Table 5. Canopy BRF may be expressed as:

$$R = R_T P_T + R_G P_G + R_{ZT}\left(1 - P_{vg} - P_T\right) + R_{ZG}\left(P_{vg} - P_G\right) \quad \text{(A1)}$$

After substitution for the probabilities discussed in [1], this may be re-written into a four coefficient expression :

Full Model:	Full Model (Kernel Form):	
$R = R_{zt} \times \left[\left(1 - P_{vg}\right) - F\left(1 - P_{ig}\right) - P_{Tf}\left(1 - F\right)\left(1 - P_{vg}\right)\right]$	$R = R_{zt} \times k_1$	(A2)
$+ R_{zg} \times \left[P_{vg} - P_{ig}\left\{F\left(1 - P_{vg}\right) + P_{vg}\right\}\right]$	$+ R_{zg} \times k_2$	(A3)
$+ R_t \times \left[F\left(1 - P_{ig}\right) + P_{Tf}\left(1 - F\right)\left(1 - P_{vg}\right)\right]$	$+ R_t \times k_3$	(A4)
$+ R_g \times \left[P_{ig}\left\{F\left(1 - P_{vg}\right) + P_{vg}\right\}\right]$	$+ R_g \times k_4$	(A5)

Where the proportions of viewed and illuminated background (P_{vg}, P_{ig} respectively) are given by:

$$P_{(i,v)g}\left(\theta_{(i,v)}\right) = \exp\left(\frac{-G(\theta) \cdot LAI \cdot \Omega}{\cos\left(\theta_{(i,v)}\right)}\right) \quad \text{(A6)}$$

The probability of viewing within-crown solar-illuminated foliage is expressed as:

$$P_{Tf} = \Omega \cdot \Gamma(\xi)\left(\frac{G(\theta)}{\sin\left(\theta_i + 15^\circ\right) + \sin\left(\theta_v + 15^\circ\right)}\right) \quad \text{(A7)}$$

where a first-order geometric scattering phase function provided by Chen and Leblanc [2] is used here:

$$\Gamma(\xi) = \left(1 - \frac{C_p \xi}{\pi}\right), \quad C_p = 0.75 \quad \text{(A8)}$$

An angular hot spot correlation function is also introduced in [1] as follows:

$$F = \exp\left(\frac{-2\pi\xi}{\xi_{F\max}} \left[1 - \exp\left\{ \frac{-G(\theta) \cdot LAI \cdot \Omega}{\cos(\theta_v)} \right\} \right] \right) \tag{A9}$$

where:

$$\xi_{F\max} = \frac{\frac{1}{2}(\pi - \theta_i)\left(1 - \left[\frac{\theta_i}{\pi - \theta_i} \right]^2 \right)}{1 + \frac{\theta_i}{\pi - \theta_i}\cos(\phi_H)} \tag{A10}$$

$$\phi_H = \tan^{-1}\left(\frac{\theta_v \cdot |\sin(\phi)|}{\theta_v \cdot \cos(\phi) - \theta_i} \right) \tag{A11}$$

Canopy multiple scattering is expressed as ratios of sunlit to shaded reflectance for the overstorey and understorey.

$$\frac{R_{ZT}}{R_T} = C_m \cdot F_{dt} \tag{A12}$$

$$\frac{R_{ZG}}{R_G} = C_m \cdot F_{dg} \tag{A13}$$

AKNOWLEDGEMENT

We would like to thank S. Leblanc for his constructive comments, discussions, and assistance in editing that contributed to this paper. We would also like to acknowledge P. Bicheron and M. Leroy for contributing POLDER data and D. Deering for contributing PARABOLA data used in this paper.

REFERENCES

[1] H.P. White, J.R. Miller, and J.M. Chen, "Four-scale linear model for anisotropic reflectance (FLAIR) for plant canopies. I: Model description and partial validation", *IEEE Trans. GeoSci. Remote Sens.*, **39**(5): 1072-1083, 2000.

[2] J.M. Chen and S.G. Leblanc, "A four-scale bidirectional reflectance model based on canopy architecture", *IEEE Trans. GeoSci. Remote Sens.*, **35**(5): 1316-1337, 1997.

[3] W. Wanner, X. Li, and A.H. Strahler, "On the derivation of kernels for kernel-driven models of bidirectional reflectance", *J. Geophys. Res.*, **100**(D10): 21077-21089, 1995.

[4] A. Wu, Z. Li, and J. Cihlar, "Effect of land cover type and greenness on advanced very high resolution radiometer reflectance: analysis and removal", *J. GeoPhys. Res.*, **100**(D10): 9179-9192, 1995.

[5] J. Cihlar, D. Manak, and N. Voisin, "AVHRR bidirectional reflectance effect and compositing", *Remote. Sens. Environ.*, **48**: 77-88, 1994.

[6] S.G. Leblanc, P. Bicheron, J.M. Chen, M. Leroy, and J. Cihlar, "Investigation of radiative transfer in boreal forests with an improved 4-scale model and airborne POLDER data", *IEEE Trans. Geosci. Remote Sens.*, **37**: 1396-1414, 1997.

[7] B. Hu, W. Lucht, X. Li, and A.H. Strahler, "Validation of kernel-driven semiempirical models for the surface bidirectional reflectance distribution function of land surfaces", *Remote Sens. Environ.*, **62**: 201-214, 1997.

[8] S. Liang, "Narrowband to broadband conversions of land surface albedo. I. Algorithms", *Remote Sens. Environ.*, **76**: 213-238, 2001

[9] H.P. White, S.G. Leblanc, J. Cihlar, and J. Chen, "Mapping Biophysical Parameters with Modelled and Inverted Functions from Directional Satellite Measurements.", *Proc. 17th Can. Symp. Remote Sensing*, Laval University, Quebec.

[10] BOREAS, Boreal Ecosystem Atmosphere Study Experiment Plan Version 3.0, P.J. Sellers et al. (eds), NASA Goddard Space Flight Centre, Greenbelt, MD, 4 volumes, 1994.

[11] P.J. Sellers, F. Hall, H. Margolis, B. Kelly, D. Baldocchi, G. den Hartog, J. Cihlar, M.G. Ryan, B. Goodison, P. Crill, K.J. Ranson, D. Lettenmaier, D.E. Wickland, "The Boreal ecosystem-atmosphere study (BOREAS): An overview and early results from the 1994 field year." *Bull. Am. Met. Soc.* **76**(9): 1549–1577, 1995.

[12] P-Y. Dechamps, F.M. Bréon, M. Leroy, A. Podaire, A. Bricaud, J.-C. Buriez, and G. Sève, "The POLDER mission: Instrumental characteristics and scientific objectives.", *IEEE Trans. Geosci. Remote Sensing*. **32**: 598-613.

[13] D.W. Deering, S.P. Ahmad, T.F. Eck, and B.P. Banerjee, "Temporal attributes of the bi-directional reflectance for three boreal forest canopies.", *Proc. Int. Geosci. Remote Sens. Symp.*, **95** : 1239-1241, 1995.

[14] D.W. Deering, T.F. Eck, and B. Banerjee, "Characterization of the reflectance anisotropy of three boreal forest canopies in spring-summer.", *Remote Sens. Environ*. **60**:71-82., 1999.

[15] J. R. Miller, J. Freemantle, P. Shepherd, L. Gray, N. O'Neill, A. Royer, and E. Senese, "Development of CASI to meet the needs of BOREAS science", *Proc. 17th Can. Symp. Remote Sensing*, Saskaton, SK, 1995.

[16] H. Peter White, *Investigations of Boreal Forest Bidirectional Reflectance Factor (BRF)*, Ph.D. Thesis, Graduate Programme in Physics and Astronomy, York University, Ontario., 1999.

[17] H.P. White, J.R. Miller, J.M. Chen, and D.R. Peddle, "Seasonal change in mean understorey reflectance for BOREAS sites: Preliminary results", in *Proc. 17th Can. Symposium on Remote Sensing*, pp. 189-194, 1995.

[18] J.M. Chen and S.G. Leblanc, "A geometrical multiple scattering scheme to be used in geometric optical models", *(in press) IEEE Trans. Geosci. Remote Sens.*, 2001.

[19] E.D. Vermote, J.L. Deuze, and J.J. Morcrette, "Second simulation of the satellite signal in the solar spectrum: an overview.", *IEEE Trans. Geosci. Remote Sens.*, **34**, 1996.

[20] B. Hu, K. Innanen, J. Miller, "Retrieval of Leaf Area Index and Canopy Closure from CASI Data over the BOREAS Flux Tower Sites", *Remote Sens. Environ.*, **74**(2) : 255-274, 2000.

[21] N.T. O'Neill, F. Zagolski, M. Bergeron, A. Royer, J. Miller, J. Freemantle, "Atmospheric correction of CASI images acquired over the BOREAS southern study area.", *Can. J. Remote Sens.*, **23**, 1997.

[22] E.M. Middleton, E.A. Walter-Shea, M.A. Mesarch, S.S. Chan, and R.J. Rusin, "Optical properties of canopy elements in black spruce, jack pine, and aspen stands in Saskatchewan, Canada.", *Can. J. Remote Sens.*, vol. 23., pp. 188-199, 1996.

[23] J.M. Chen, "Optically-based methods for measuring seasonal variations of leaf area index in boreal conifer stands", *Agric. For. Meteorol.*, vol. 80, pp. 138-163, 1996.

[24] R. Lacaze and J-L. Roujean "G-function and HOt SpoT (GHOST) reflectance model. Application to multi-scale airborne POLDER measurements", *Remote Sens. Environ.*, (accepted – 2001).

Figure 1

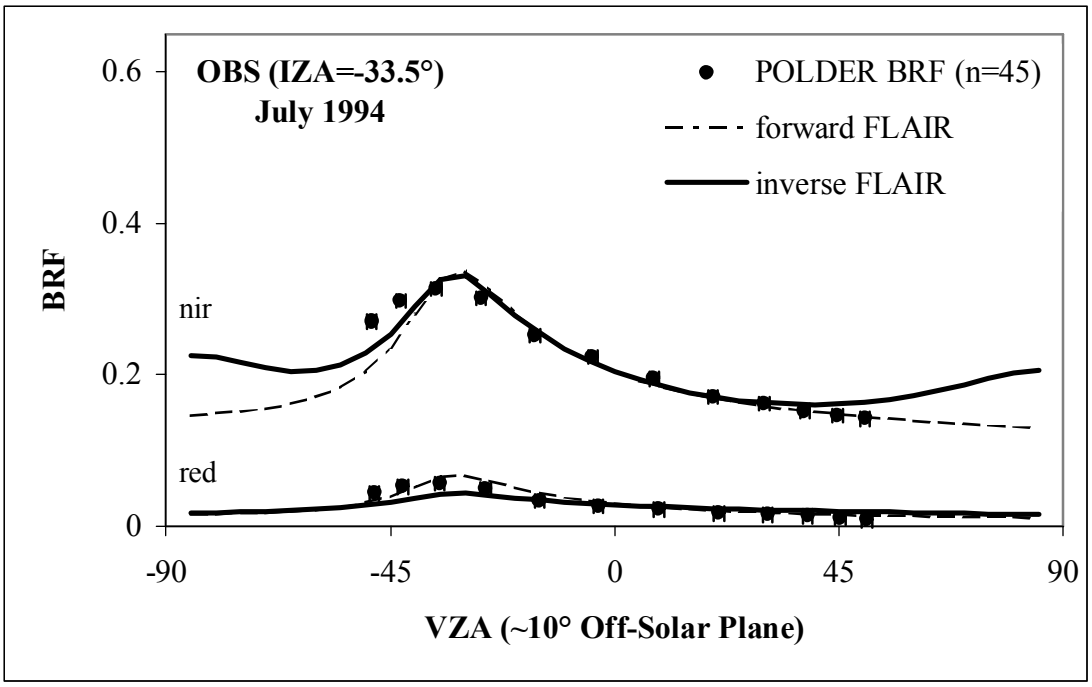

a

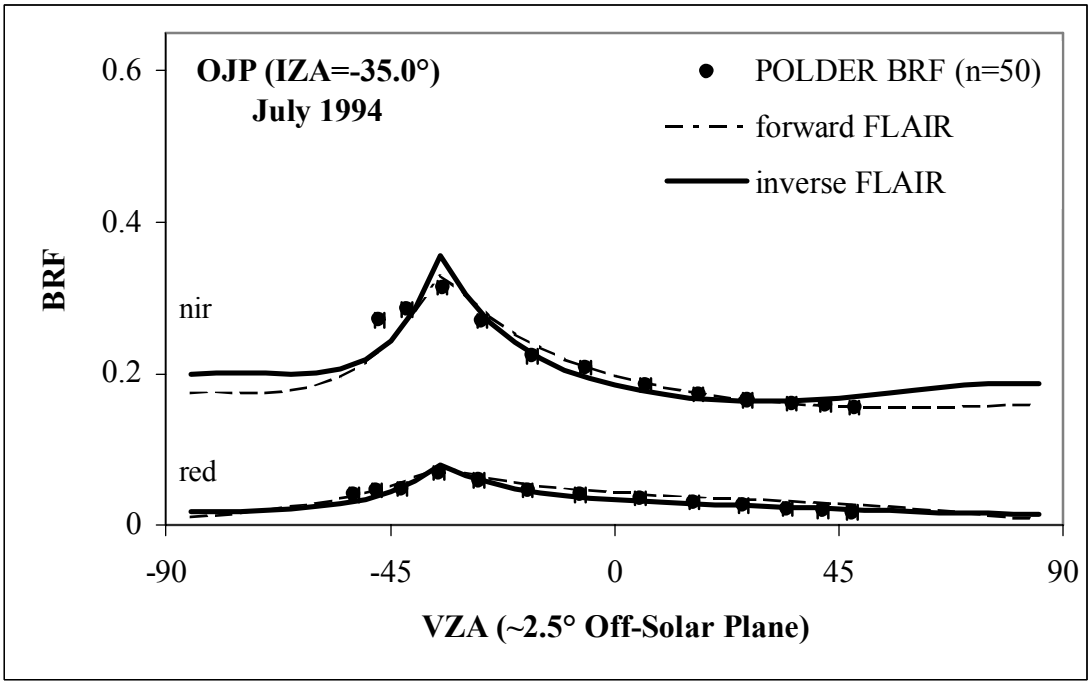

b

Nominal input model data from observed field data for BOREAS '94 Tower Flux Sites.

Figure 2

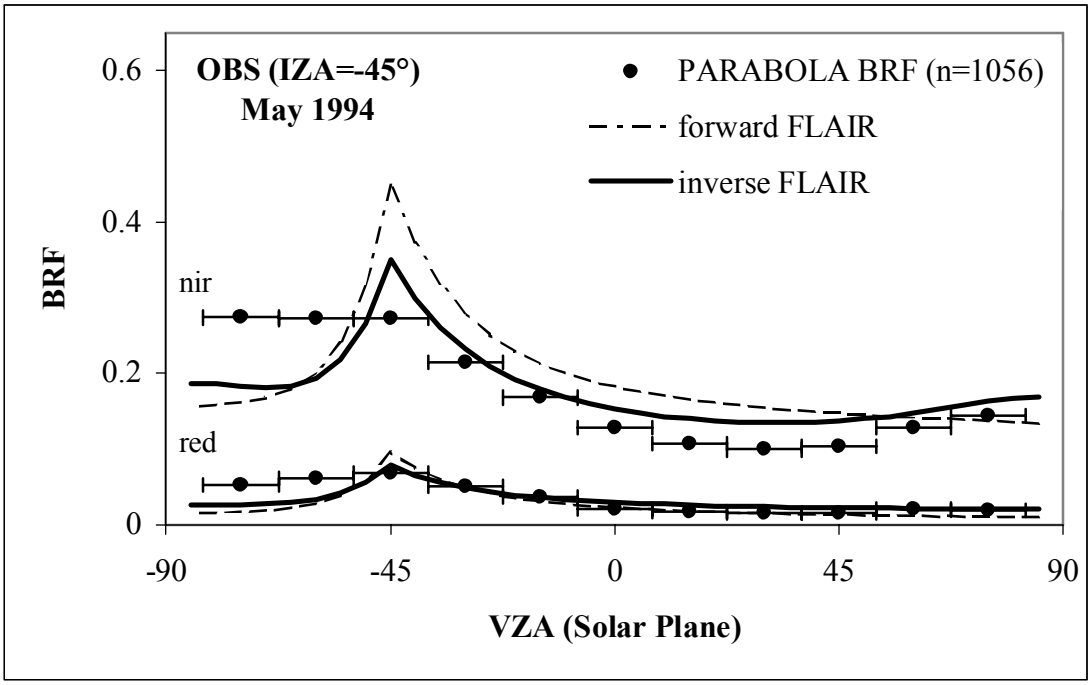

a

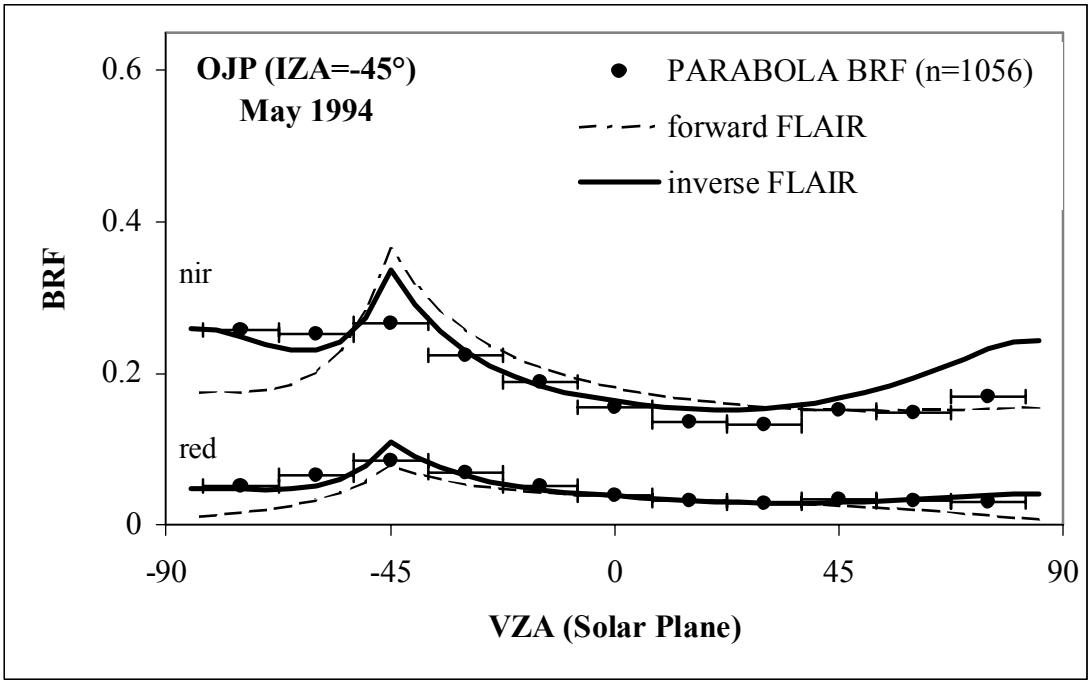

b

Canopy properties determined for the POLDER SSA-OBS and SSA-OJP BRF uni-θ_i data sets by FLAIR inversion. RMSE and r_{cc} values are determined by comparing FLAIR functions to observed BRF data. Property value ranges indicate the range of the minimum constraint volume determined during the inversion process. Arrows indicate these ranges from low → high L_e. N refers to the number of view angles per band used in the inversion.

Figure 3

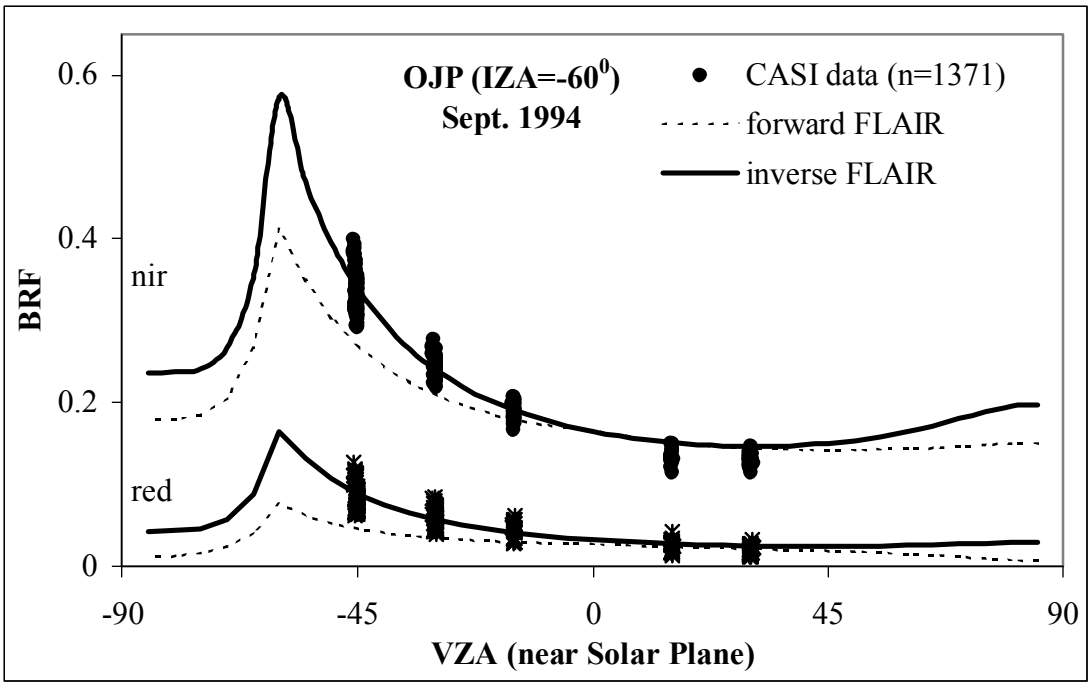

a

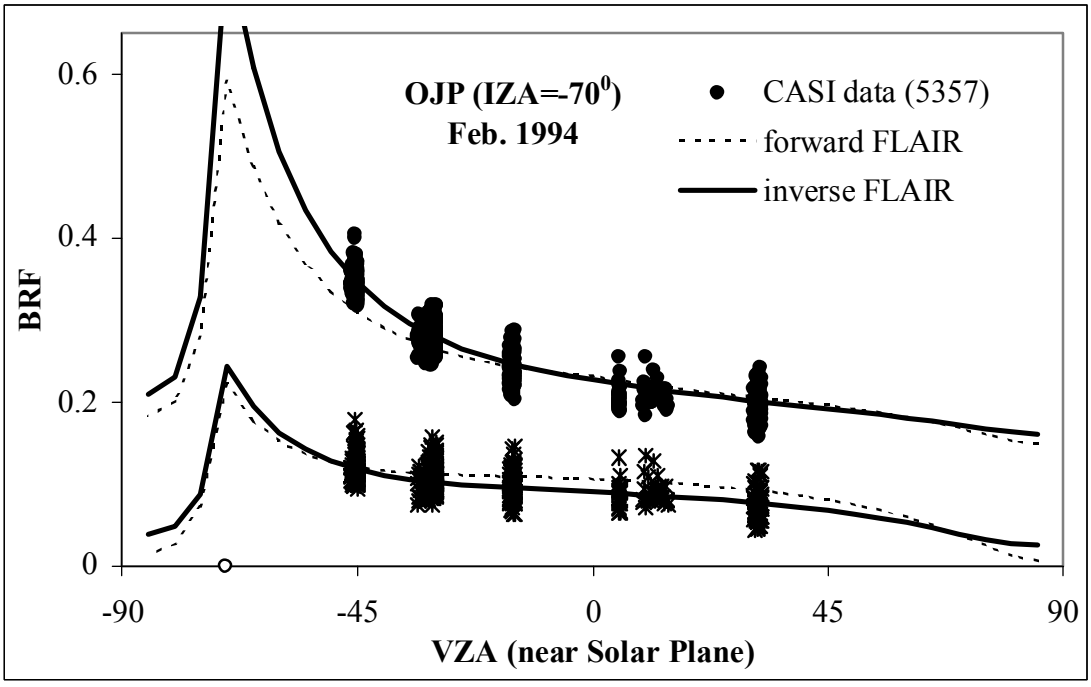

b

Canopy properties determined for the PARABOLA SSA-OBS and SSA-OJP BRF multi-θ_i data sets by FLAIR inversion. RMSE and r_{cc} values are determined by comparing FLAIR functions to observed BRF data.

Figure 4

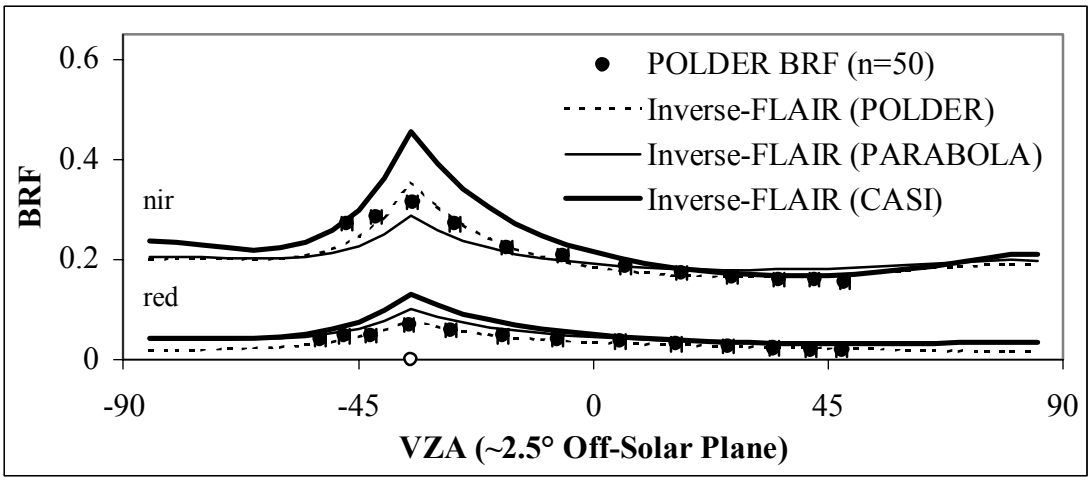

a

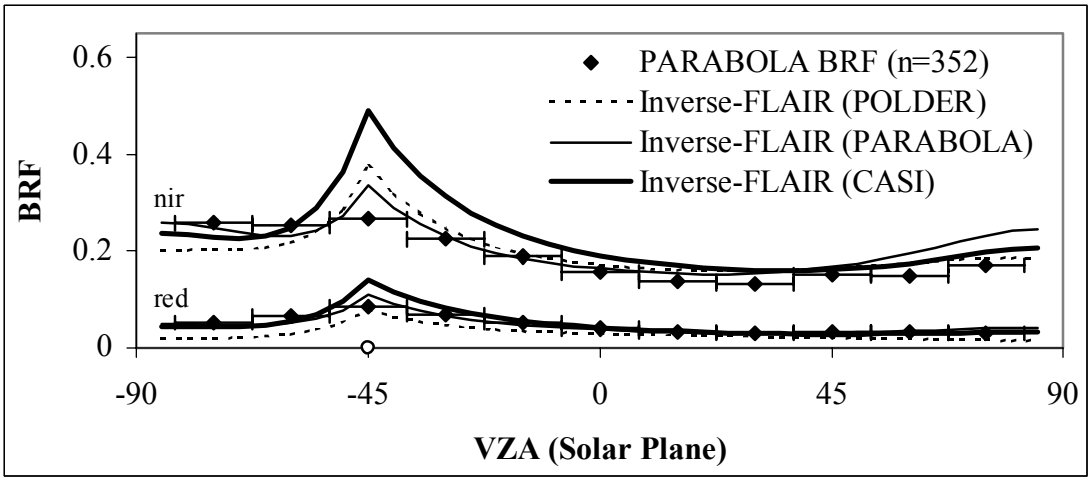

b

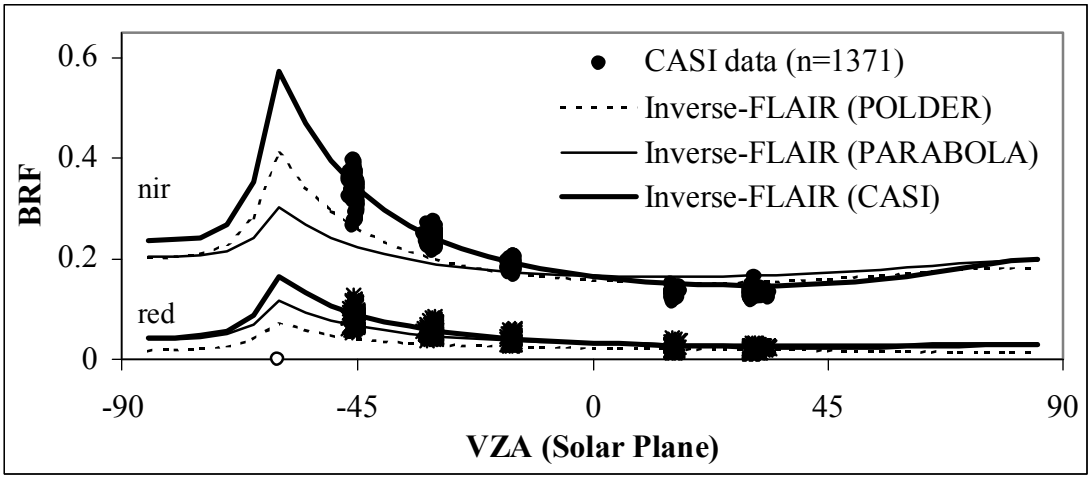

c

Canopy properties determined for the CASI late summer and mid-winter SSA-OJP BRF multi-θ_i data sets by FLAIR inversion. RMSE and r_{cc} values are determined by comparing FLAIR functions to observed BRF data.

Table 1

	OBS	YJP	OJP
Site Location			
Latitude	53.985^0	53.975^0	53.916^0
Longitude	-105.12^0	-104.65^0	-104.69^0
Foliage Distribution			
Ω_E * (clumping index)	0.80	0.83	0.77
γ_E * (leaf to shoot index)	1.44	1.38	1.51
$G(\theta)$	0.5	0.5	0.5
LAI (L_e)	4.5 (2.5)	2.7 (1.6)	2.2 (1.1)
Reflectance Properties			
R_G (red)	0.04	0.05	0.09
$C_m F_{dg}$ (red)	0.05	0.08	0.033
R_T (red)	0.11	0.05	0.07
$C_m F_{dt}$ (red)	0.027	0.10	0.043
R_G (NIR)	0.25	0.15	0.17
$C_m F_{dg}$ (NIR)	0.44	0.53	0.53
R_T (NIR)	0.50	0.53	0.53
$C_m F_{dt}$ (NIR)	0.22	0.36	0.25

Adapted from Leblanc et al., 1999. *Adapted from Chen, 1996.

Nominal input model data from observed field data for BOREAS '94 Tower Flux Sites.

Table 2

POLDER	SSA-OBS (N=23)		SSA-OJP (N=23)	
	Red (670 nm)	NIR (864 nm)	Red (670 nm)	NIR (864 nm)
C_mF_{dt}	0.14 → 0.15	0.24 → 0.27	0.15 → 0.16	0.37 → 0.38
C_mF_{dg}	0.17 ← 0.30	0.15 → 0.50	0.26 → 0.30	0.25 → 0.71
R_t	0.07 → 0.07	0.55 ← 0.68	0.07 ← 0.10	0.42 ← 0.46
R_g	0.03 → 0.06	0.08 ← 0.13	0.04 → 0.11	0.02 ← 0.12
L_e	1.20 → 2.46		1.90 → 3.19	
RMSE	0.011 → 0.015		0.008 → 0.009	
r_{cc}	0.991 ← 0.994		0.995 ← 0.996	

Canopy properties determined for the POLDER SSA-OBS and SSA-OJP BRF uni-θ_i data sets by FLAIR inversion. RMSE and r_{cc} values are determined by comparing FLAIR functions to observed BRF data. Property value ranges indicate the range of the minimum constraint volume determined during the inversion process. Arrows indicate these ranges from low → high L_e. N refers to the number of view angles per band used in the inversion.

Table 3

PARABOLA	SSA-OBS (N=1056)			SSA-OJP (N=1056)		
	Red (662 nm)	NIR (864 nm)	MIR (1658 nm)	Red (662 nm)	NIR (864 nm)	MIR (1658 nm)
C_mF_{dt}	0.15	0.30	0.22	0.20	0.59	0.28
C_mF_{dg}	0.30	0.24	0.26	0.30	0.34	0.42
R_t	0.10	0.49	0.39	0.13	0.32	0.50
R_g	0.03	0.12	0.04	0.03	0.21	0.02
L_e	1.42			1.94		
RMSE	0.056			0.036		
r_{cc}	0.815			0.896		

Canopy properties determined for the PARABOLA SSA-OBS and SSA-OJP BRF multi-θ_i data sets by FLAIR inversion. RMSE and r_{cc} values are determined by comparing FLAIR functions to observed BRF data.

Table 4

CASI	FFC-W SSA-OJP (N=5357)		IFC-3 SSA-OJP (N=1371)	
	Red (670 nm)	NIR (864 nm)	Red (670 nm)	NIR (864 nm)
C_mF_{dt}	0.09	0.18	0.09	0.23
C_mF_{dg}	0.10	0.17	0.05	0.30
R_t	0.19	0.75	0.22	0.75
R_g	0.65	0.79	0.02	0.10
L_e	1.46		1.30	
RMSE	0.018		0.025	
r_{cc}	0.865		0.892	

Canopy properties determined for the CASI late summer and mid-winter SSA-OJP BRF multi-θ_i data sets by FLAIR inversion. RMSE and r_{cc} values are determined by comparing FLAIR functions to observed BRF data.

Table 5

BRDF	Bi-directional Reflectance Distribution Function
BRF	Bi-directional Reflectance Factor
C_m	Fraction of downwelling irradiance due to multiple scattering within the canopy.
C_p	Foliage asymmetry factor.
F	Hot spot correlation function.
F_{dt}, F_{dg}	Fraction of downwelling irradiance due to diffuse sky irradiance as viewed near the top of the canopy and near the bottom of the canopy respectively.
$\Gamma(\xi)$	First-order scattering (geometric shadow) phase function of a foliage element (i.e., needle shoot).
$G(\theta)$	Projection of unit leaf area.
ϕ_i	Solar Illumination Azimuth Angle.
θ_i	Solar Illumination Zenith Angle.
k_i	FLAIR kernel designation.
LAI	Leaf Area Index
Ω	Nonrandomness factor. (Ratio of Ω_E to γ_E).
P_{ig}, P_{vg}	Probably of viewing the understorey.
P_T, P_G	Proportion of sunlit canopy and sunlit understorey respectively.
P_{Tf}	Probability of viewing illuminated foliage when the view and illumination perspectives are not correlated.
P_{ti}	Proportion of observed tree crown that is illuminated
R_G, R_T, R_{ZG}, R_{ZT}	Mean reflectance factor of the sunlit understorey, sunlit crown, shaded understorey, and shaded crown respectively.
ϕ_v	View Azimuth Angle (often given relative to the IAA).
θ_v	View Zenith Angle
ξ	Angle difference between the Sun and viewer. (scattering angle)
Z_T, Z_G	Proportion of shaded crown and shaded understorey respectively.
ZWH	Zenithal width of the hot spot

Symbol nomenclature used in this paper.

Bios

H. Peter White received his B.Sc. degree in Physics and Astronomy from Saint Mary's University in 1988 and his M.Sc. (1994) and Ph.D. (1999) in Physics and Astronomy from York University.

He is currently a Research Scientists at Natural Resources Canada, Canadian Centre for Remote Sensing (CCRS) in Ottawa, Ont. His remote sensing interests have included Jovian planetary atmospheric composition and modelling optical bidirectional reflectance of boreal ecosystems. Current research is focused on applications development of modelling and retrieval of biophysical parameters of vegetative surfaces using optical remote sensing techniques.

John R. Miller received a B.E. degree (Physics) from the University of Saskatchewan, Saskatoon, in 1963, and both M.S.c. (1966) and Ph.D. (1969) degrees in space physics from the same university, studying the aurora borealis using rocket-borne radiometers.

He then spent two years on a postdoctoral fellowship at the Herzberg Institute at the National Research Council in Ottawa. In 1971 he went to work as a Project Scientist at York University. He is currently Professor of Physics and Astronomy at York University and is Co-director of the Earth Observations Laboratory of the Centre for Research in Earth and Space Technology (CRESTech). His remote sensing interests include atmospheric correction and interpretation of water colour reflectance and canopy reflectance. Over the past decade his primary focus has been on the application of reflectance spectroscopic techniques in remote sensing using imaging spectrometers.

Jing M. Chen received a B.Sc. degree in 1982 from Nanjing Institute of Meteorology, China, and a Ph.D. degree in 1986 from the University of Reading, Reading, UK.

He is currently a Research Scientist at the Canadian Centre for Remote Sensing (CCRS) in Ottawa, Ont., and a Professor in the Department of Geography, University of Toronto, Ont. His main research interests have been in turbulent and radiative transfer processes associated with plant canopies. He is currently engaged in research on applications of optical and microwave remote sensing techniques to boreal ecosystems. Research topics include radiation modelling, biophysical parameter retrieval, and modelling net primary productivity and carbon cycle.